UNIVERSITY OF CALIFORNIA, SAN DIEGO

The phosphoprotein Rppa09976 bridges peroxisomal and isolation membranes during pexophagy

A thesis submitted in partial satisfaction of the requirements for the degree of Master of Science

in

Biology

by

Pouya Lotfi

Committee in charge:

Suresh Subramani, Chair
Immo E. Scheffler
Jayant Ghiara

2010

The thesis of Pouya Lotfi is approved, and is acceptable in quality and form for publication on microfilm and electronically:

Chair

University of California, San Diego

2010

TABLE OF CONTENTS

Signature Page……iii

Table of Contents……iv

List of Figures……v

List of Tables……vii

Acknowledgements……viii

Abstract……x

Chapter I: Introduction……1

Chapter II: Rppa09976 undergoes a protein modification during peroxisome biogenesis……12

Chapter III: Rppa09976 interactions……30

Chapter IV: Rppa09976 mutants……43

Chapter V: Conclusion……55

LIST OF FIGURES

Figure1-1: Modes of general autophagy and pexophagy……..……..8

Figure 2-1: Functional domains and motifs of Rppa09976……...21

Figure 2-2: Rppa09976 modification…….…...22

Figure 2-3: PAP dephosphorylates Rpp09976-HA in cell
lysates prepared by glass beads…….……23

Figure 2-4: NaF preserves the higher molecular weight,
phosphorylated bands of Rppa09976-HA and Pex14 in glass bead lysates…..…...24

Figure 2-5: PAP completely removes all modified forms of
Rppa09776 preserved by NaF…….....25

Figure 2-6: Predicted phosphorylation sites of Rppa09976……... 26

Figure 2-7: Large scale affinity purification of Rppa09976-HA……....27

Figure 2-8: Predicted and found phosphorylation sites of Rppa09976……...28

Figure 3-1: Co-immunoprecipitation of Rppa09976-HA and Pex3
during methanol adaptation…….……...37

Figure 3-2: Co-immunoprecipitation of Pex3 with Rppa09976-HA
under micropexophagy conditions……..…….38

Figure 3-3: Rppa09976-HA co-immunoprecipitated with mCherry-Atg8
under micropexophagy conditions…….39

Figure 3-4: Rppa09976-HA co-immunoprecipitated with Atg30-GFP
under micropexophagy conditions……..…..40

Figure 3-5: Rppa09976 interacts with Pex3, Atg8 and Atg30, perhaps guiding
the growing MIPA around peroxisomes tagged for degradation……...41

Figure 4-1: Localization of mutated versions of Rppa09976 in

peroxisome-biogenesis conditions…….49

Figure 4-2: Pexophagy assay of mutated versions of Rppa09976……..50

Figure 4-3: Co-immunoprecipition of Rppa09976-HA with mCherry-Atg8 under micropexophagy conditions……..51

Figure 4-4: Co-immunoprecipition of single and double mutated LIR Rppa09976-HA with mCherry-Atg8 under micropexophagy conditions……. 52

Figure 4-5: Pexophagy assay of 1st LIR mutated Rppa09976-HA…….53

LIST of TABLES

Table 2-1. *P. pastoris* strains and plasmids used in this study……..…..20

ACKNOWLEGEMENTS

I would like to thank several people for supporting me and assisting me during my years in the laboratory. I thank Taras for teaching me science and designing my experiments. Also, I would like to thank Katharine for teaching me laboratory techniques. I appreciate Professor Subramani for letting me to study and work in the lab. Additionally, I am grateful for the help from my colleagues, including Jean-Claude, Gaurav and Whitney.

Chapter 1 is currently being prepared to submit for publication of the material. Lotfi, Pouya; Ozeki, Katharine; Nazarko, Taras Y; and Subramani, Suresh. The thesis author was the primary investigator and author of this paper.

Chapter 2 is currently being prepared to submit for publication of the material. Lotfi, Pouya; Ozeki, Katharine; Nazarko, Taras Y; and Subramani, Suresh. The thesis author was the primary investigator and author of this paper.

Chapter 3 is currently being prepared to submit for publication of the material. Lotfi, Pouya; Ozeki, Katharine; Nazarko, Taras Y; and Subramani, Suresh. The thesis author was the primary investigator and author of this paper.

Chapter 4 is currently being prepared to submit for publication of the material. Lotfi, Pouya; Ozeki, Katharine; Nazarko, Taras Y; and Subramani, Suresh. The thesis author and Ozeki, Kahtherine contributed equally to this paper.

Chapter 5 is currently being prepared to submit for publication of the material. Lotfi, Pouya; Ozeki, Katharine; Nazarko, Taras Y; and Subramani, Suresh. The thesis author and Ozeki, Kahtherine contributed equally to this paper.

ABSTRACT OF THE THESIS

The phosphoprotein Rppa09976 bridges peroxisomal and isolation membranes during pexophagy

by

Pouya Lotfi

Master of Science in Biology

University of California, San Diego, 2010

Professor Suresh Subramani, Chair

Peroxisomes are important single membrane organelles which are required for certain metabolic pathways. In yeast, *Pichia pastoris*, peroxisomes are degraded by selective autophagy pathway termed pexophagy. Autophagy is process whereby proteins and organelles are delivered to the vacuole and degraded. Previous studies indicated Atg30 as the receptor for pexophagy, which interacts with the autophagic machinery (Atg11 and Atg17) as well as peroxisomal membrane (Pex3 and Pex14). However, unlike other selective autophagy receptors, Atg30 does not interact with Atg8, a major

component of the isolation membrane that sequester peroxisomes during pexophagy. Here, we found the missing link, a novel peroxisomal membrane protein Rppa09976, which bridges peroxisomal (Pex3 and Atg30) and isolation (Atg8) membranes. Rppa09976 is phosphoprotein that contains an N-terminal acyl-CoA binding domain, three putative Atg8 binding sites and two transmembrane domains. Rppa09976 is expressed in methanol medium and phosphorylated upon arrival to peroxisomes from ER. We purified the Rppa09976-HA fusion protein and mapped 21 phosphorylation sites by mass spectrometry. The functional role of Rppa09976 phosphorylation awaits further studies. We showed that two of the three putative Atg8 binding sites at the N-terminal of the protein are required for Atg8 binding and pexophagy. Point mutation of the conserved acyl-CoA binding site also leads to a pexophagy defect. Hence, we propose that Rppa09976 provides acyl-CoA for the growing isolation membranes that sequester peroxisomes.

Chapter I: Introduction

A. Autophagy

Autophagy is an intracellular process in eukaryotic cells whereby cytoplasmic components ranging from macromolecules to organelles are degraded by lysosomes to maintain a balance between synthesis, degradation and subsequent recycling of cellular building blocks. There are two subtypes of autophagy: macroautophagy and microautophagy. In macroautophagy, double-membrane structures known as isolation membranes are formed (probably from the endoplasmic reticulum) that sequester cytoplasmic components non-selectively. After formation of these vesicles, known as autophagosomes, this compartment is delivered to lysosomes for degradation, by fusion of the outer membrane of autophagosomes with the lysosomal membrane. In microautophagy, lysosomal invaginations take up cytoplasmic components for degradation (Figure 1-1). Although autophagy takes place under basal conditions to breakdown superfluous cell components, it also happens to a higher extent in response to stresses, such as starvation, to maintain homeostasis (1).

B. Conservation of autophagy across species

To date 32 AuTophaGy-related (ATG) genes have been identified. Most of these genes are conserved from yeast to higher eukaryotes. The processes of autophagy are also conserved from yeast to higher eukaryotes; one minor difference is that yeast use vacuoles for degradation instead of lysosomes. Autophagy can easily be induced in yeast

by nutritional starvation and since yeast is readily cultured, it has served as a great model organism to study autophagy. Using yeast, particularly *S. cerevisiae,* led to knowledge regarding the multiple steps of macroautophagy. Each step requires a set of Atg proteins. Broadly these steps include: (i) induction of autophagy; (ii) recognition of autophagic cargo; (iii) autophagosome formation; (iv) fusion of autophagosome to the vacuole and breakdown; (v) recycling of building blocks (2). Unraveling components of the autophagy molecular machinery in yeast has led to an explosion in research on autophagy in higher eukaryotes, particularly humans.

C. Significance of autophagy in human disease

Deficits in autophagy have been linked to variety of human diseases including cancer, neurodegenerative disorders such as Alzheimer's, Parkinson's and Huntington's disease (3). Neurodegenerative diseases mentioned above lead to accumulation of protein aggregates in the cytosol. In Huntington's disease, where abnormal levels of polyglutamine aggregates disrupt cell function, autophagy is induced to reduce the amount of aggregated protein and alleviate the symptoms of the disease (1). Autophagy has also been implicated as a tumor suppressor mechanism. In some cancer cells reduced autophagic activity is observed. In these cells, stimulation of autophagy by exogenous expression of BECLIN 1 (autophagy inducer gene) leads to inhibition of tumorigenesis (4). Autophagy also plays roles in the immune system. In the adaptive immune response, autophagy is believed to have a role in mediating the presentation of endogenous antigens by MHC class II, which is unusual in that MHC class II are traditionally believed to present exogenous antigens (5). Autophagy is also linked to innate immunity specifically

during bacterial invasion where the human protein, Atg16L1, is recruited to the site of infecting bacteria by NOD2 (bacteria receptor) where it starts the process of autophagosome formation to degrade the bacteria (2). Taken together, autophagy has obvious roles in multiple human diseases, so an understanding of autophagy mechanisms may lead to therapeutic treatment for autophagy related diseases.

D. Selective autophagy

Apart from non-selective macroautophagy, there are other related forms of autophagy consisting of many selective subtypes such as the Cvt (cytoplasm to vacuole targeting) pathway, mitophagy, ER phagy, ribophagy, micronucleophagy and pexophagy. The Cvt pathway is a biosynthetic pathway that uses the autophagy machinery to selectively deliver the precursor of the protein, Aminopeptidase I (PreApeI), to the vacuole. PreApe1 is synthesized in cytosol and oligomerizes, and is then recognized by its receptor, Atg19, which tags the cargo for delivery to vacuole in Cvt vesicles (6). In mitophagy, damaged mitochondria are recognized by the newly discovered protein, Atg32, which tags them for degradation (7). In ER phagy, ribophagy and micronucleophagy, parts of the ER, ribosomes or nucleus are degraded by autophagy. In pexophagy, specifically in *Pichia pastoris*, peroxisomes are tagged by Atg30 for degradation upon induction of pexophagy (8).

All selective modes of autophagy known to date require interaction of a specific receptor protein with Atg8, a protein present on the isolation membrane. This interaction happens through a putative LIR motif (Atg8/LC3-interacting region) that has been identified on Atg19 and Atg32. However, this LIR motif (WxxL) does not exist on

Atg30, nor has an interaction between Atg30 and Atg8 been found. Atg32, the receptor for mitophagy, directly interacts with Atg8. In the Cvt pathway, even though Atg19 interacts with Atg8, Atg19 still requires an adaptor protein, Atg11, which enables it to complete interaction with the autophagic machinery (6). Perhaps the pexophagy receptor also requires an adaptor protein to complete its interactions with autophagy machinery.

E. Peroxisomes

Peroxisomes are single membrane organelles that have interesting and unique features. They are involved in the β-oxidation of fatty acids, decomposition of reactive oxygen species, production of penicillin in certain fungi, and photorespiration in plants. Peroxisome biogenesis defects in human lead to disorders such as Zellweger syndrome, rhizomelic chondrodysplasia punctata and neonatal adrenoleukodystrophy (9).

Peroxisomal proteins are encoded by nuclear genes and those involved in peroxisome biogenesis are termed peroxins (Pex). Peroxisomes contain many enzymes which are imported post-translationally, in the folded or oligomeric state, through a translocon that adjusts its diameter depending on incoming protein size (10). Matrix proteins are imported via peroxisomal targeting signals (PTS1 or PTS2). Pex5 and Pex7 recognize PTS1 and PTS2 sequences, respectively, and bring these peroxisomal matrix proteins to the translocon (11). However, several, if not all, peroxisomal membrane proteins (PMPs) are transported to peroxisomes via the ER. First PMPs are targeted to ER and then vesicles containing PMPs leave the ER and fuse with pre-existing peroxisomes, thereby allowing their growth prior to division (12). At early stages of this pathway, Pex3 an essential peroxisomal protein is targeted to the ER. Then Pex3

segregates to a pre-peroxisomal template, which is followed by Pex19, PMP receptor, recruitment (13).

F. Macropexophagy and Micropexophagy

Peroxisomes are easily induced and grow in number and size in response to environmental or physiological conditions in order to help the cell adapt to new conditions, in a species dependent manner. For example, in our model organism, the methylotrophic yeast *P. pastoris*, peroxisomes are rapidly induced in methanol/oleate media and upon prolonged induction peroxisomes occupy a large fraction of the cell volume in order to metabolize methanol/oleate. Peroxisomes are rapidly reduced in number when they are not needed. In our case, the transfer of cells from methanol to ethanol or glucose (with or without nitrogen) leads to two different modes of degradation of peroxisomes: macropexophagy and micropexophagy, respectively (Figure 1-1). These are modified autophagy pathways where peroxisomes are selectively recognized, sequestered and degraded through vacuolar proteases and lipases (14).

Micropexophagy sequesters the peroxisomes by invagination of sequestering arms of the vacuolar membrane around a cluster of peroxisomes. The complete sequestration of peroxisomes by micropexophagy requires a membranous structure called the micro-pexophagy specific apparatus (MIPA), which is thought to fuse with the extended vacuolar sequestering membranes (VSMs). Fusion of VSM and MIPA around the sequestered peroxisomes leads to engulfment of peroxisomes by the vacuole. In macropexophagy, peroxisomes are sequestered, one at a time by double-membrane vesicles (pexophagosomes) and delivered to the vacuole for fusion and degradation. The

isolation membrane for pexophagosome and MIPA is thought to be derived from the pexophagy-specific pre-Autophagosomal structure (PAS) which is a dot-like structure to which pexophagy proteins are recruited upon induction of pexophagy (14).

G. Pexophagy-specific proteins

To date, two strictly pexophagy specific proteins have been published, Atg30 and Atg26. Peroxisomes are tagged for degredation by Atg30. Atg30 interacts with Atg11 and Atg17 as well as the peroxisomal membrane proteins, Pex3 and Pex14. Atg30 deletion leads to block in pexophagy and over-expression of Atg30 leads to pexophagy even under basal conditions. These facts show that Atg30 is the receptor for peroxisome degradation, however, an important link between Atg30 and Atg8 remains to be seen as these two proteins do not interact. Atg30 is phosphorylated upon induction of pexophagy, or under basal conditions, if overexpressed. Atg30 phosphorylation at serine 112 is required for its interaction with Atg11 and degradation of peroxisomes (8). The other pexophagy specific protein, Atg26, is an enzyme (sterolglucosyltransferase) that converts ergosterol to ergosterol glucoside. It is required for the elongation of the PAS into the MIPA during micropexophagy. Atg26 is essential for degradation of medium sized or larger peroxisomes (15).

Recently, we found a novel pexophagy-specific protein, Rppa09976, in *P. pastoris*. This protein is induced under peroxisome biogenesis conditions and localizes to the ER first, then traffics to the peroxisome membrane. It accumulates multiple modifications on its way to peroxisomes. Deletion of Rppa09976 leads to major defect in pexophagy, which makes it an essential player of the pexophagy machinery. Furthermore,

this protein has a mammalian counterpart, MmAcbd5, which makes it even more noteworthy to study (16).

H. Goals of this thesis

Rppa09976 has two predicted transmembrane domains, an acyl-CoA binding site and Atg8 binding site. Rppa09976 localizes to peroxisomes which coincides with the appearance of a modified form of the protein. It is essential to find the nature and site of this modification as it may have a role in its localization and hence pexophagy. Since Rppa09976 is essential for pexophagy, it must interact with the autophagy machinery as well as with peroxins. We would like to find its interacting partners to help us better understand pexophagy and selective autophagy, in general. We are also interested in finding the role of the acyl-CoA binding domain as Rppa09976 may provide long chain fatty acyl-CoA for growth of the isolation membranes of the MIPA and pexhophagosomes. We are also interested in the role of the Rppa09976 transmembrane domain. This thesis will attempt to answer the aforementioned questions about Rppa09976.

Chapter 1 is currently being prepared to submit for publication of the material. Lotfi, Pouya; Ozeki, Katharine; Nazarko, Taras Y; and Subramani, Suresh. The thesis author was the primary investigator and author of this paper.

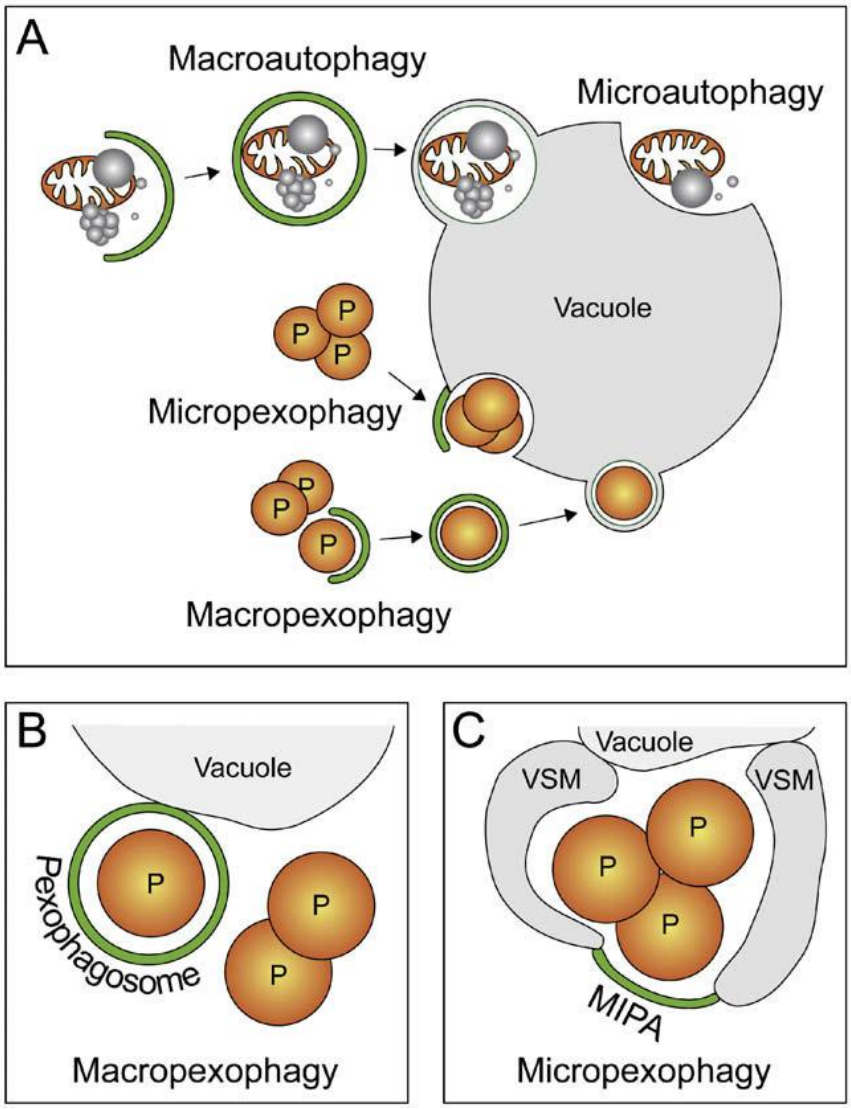

Figure 1-1: Modes of general autophagy and pexophagy. General autophagy involves sequestration and degradation of non-specific cargo (cytosolic proteins and organelles) either by engulfment into autophagosomes (macroautophagy) or by the invagination of the vacuolar membrane around these cargoes (microautophagy) (A). In an analogous fashion, pexophagy involves the engulfment of specific cargo, the peroxisomes (P) by either macro- or micropexophagy. While the formation of a pexophagosome around a peroxisome is the hallmark of macropexophagy (B), micropexophagy is morphologically

characterized by vacuolar extensions (vacuolar sequestration membranes, VSM) and the cupshaped micropexophagy apparatus (MIPA) that capture the peroxisome cluster (C) (17).

References

1. Klionsky, D. J. (2007) Autophagy: from phenomenology to molecular understanding in less than a decade, *Nat Rev Mol Cell Biol 8*, 931-937.

2. Galluzzi, L., Kepp, O., Zitvogel, L., and Kroemer, G. (2010) Bacterial invasion: linking autophagy and innate immunity, *Curr Biol 20*, R106-108.

3. Klionsky, D. J. (2005) The molecular machinery of autophagy: unanswered questions, *J Cell Sci 118*, 7-18.

4. Liang, X. H., Kleeman, L. K., Jiang, H. H., Gordon, G., Goldman, J. E., Berry, G., Herman, B., and Levine, B.gd (1998) Protection against fatal Sindbis virus encephalitis by beclin, a novel Bcl-2-interacting protein, *J Virol 72*, 8586-8596.

5. Schmid, D., Dengjel, J., Schoor, O., Stevanovic, S., and Munz, C. (2006) Autophagy in innate and adaptive immunity against intracellular pathogens, *J Mol Med 84*, 194-202.

6. Shintani, T., and Klionsky, D. J. (2004) Cargo proteins facilitate the formation of transport vesicles in the cytoplasm to vacuole targeting pathway, *J Biol Chem 279*, 29889-29894.

7. Kanki, T., and Klionsky, D. J. (2009) Atg32 is a tag for mitochondria degradation in yeast, *Autophagy 5*, 1201-1202.

8. Farre, J. C., Manjithaya, R., Mathewson, R. D., and Subramani, S. (2008) PpAtg30 tags peroxisomes for turnover by selective autophagy, *Dev Cell 14*, 365-376.

9. Subramani, S. (1998) Components involved in peroxisome import, biogenesis, proliferation, turnover, and movement, *Physiol Rev 78*, 171-188.

10. Girzalsky, W., Saffian, D., and Erdmann, R. (2010) Peroxisomal protein translocation, *Biochim Biophys Acta*.

11. Hettema, E. H., Girzalsky, W., van Den Berg, M., Erdmann, R., and Distel, B. (2000) Saccharomyces cerevisiae pex3p and pex19p are required for proper localization and stability of peroxisomal membrane proteins, *EMBO J 19*, 223-233.

12. Ma, C., and Subramani, S. (2009) Peroxisome matrix and membrane protein biogenesis, *IUBMB Life 61*, 713-722.

13. Snyder, W. B., Koller, A., Choy, A. J., and Subramani, S. (2000) The peroxin Pex19p interacts with multiple, integral membrane proteins at the peroxisomal membrane, *J Cell Biol 149*, 1171-1178.

14. Oku, M., and Sakai, Y. (2008) Pexophagy in Pichia pastoris, *Methods Enzymol 451*, 217-228.

15. Nazarko, T. Y., Farre, J. C., and Subramani, S. (2009) Peroxisome size provides insights into the function of autophagy-related proteins, *Mol Biol Cell 20*, 3828-3839.

16. Wiese, S., Gronemeyer, T., Ofman, R., Kunze, M., Grou, C. P., Almeida, J. A., Eisenacher, M., Stephan, C., Hayen, H., Schollenberger, L., Korosec, T., Waterham, H. R., Schliebs, W., Erdmann, R., Berger, J., Meyer, H. E., Just, W., Azevedo, J. E., Wanders, R. J., and Warscheid, B. (2007) Proteomics characterization of mouse kidney peroxisomes by tandem mass spectrometry and protein correlation profiling, *Mol Cell Proteomics 6*, 2045-2057.

17. Manjithaya, R., Nazarko, T. Y., Farre, J. C., and Subramani, S. (2010) Molecular mechanism and physiological role of pexophagy, *FEBS Lett 584*, 1367-1373.

Chapter II: Rppa09976 undergoes a protein modification during peroxisome biogenesis

Materials and Methods

Strains

Pichia pastoris strains used in this study are described in Table 2-1.

Induction of peroxisomes

P. pastoris cells were pre-grown to the late exponential-stationary phase in YPD medium, diluted 25 fold with fresh YPD medium and pre-grown to the early-mid exponential phase again in YPD medium. Cells were washed twice with YNB solution (1.7 g/l YNB without amino acids and ammonium sulfate) and transferred to peroxisomes-induction medium (1.7 g/l YNB without amino acids, 0.5% vol/vol methanol, 0.05% wt/vol yeast extract and 0.5% wt/vol ammonium sulfate) at an OD of 1.0 for 4 h. Histidine (50 mg/l) and/or arginine (50 mg/l) was added, when needed.

Potato acid phosphatase (PAP) treatment

15 OD of cells grown for 4 h in methanol medium were pelleted and resuspended in 500 ul of phosphate-buffered saline (PBS) containing 0.5% wt/vol SDS, and 1% vol/vol β-mercaptoethanol. Cell debris was removed by centrifugation for 1 min at 8000 g. The supernatant was boiled for 5 min. 10 ul of cell-free lysate was added to 40 ul of PAP buffer containing 50 mM MES pH 6.0, 1 mM DTT and 1 U of PAP (Boehringer) and protease inhibitors (1 mM PMSF, 1 mM protease inhibitor cocktail, 1 mM leupeptin, and 1 mM aprotinin). Samples were incubated for 2 h at 30°C. Mock controls were

treated in a similar manner, but without the addition of enzyme. Samples were mixed 1:1 with 2X SDS loading buffer and boiled for 5 min prior to SDS–PAGE and western blotting (1).

NaF treatment

Cells were grown for 4 h in methanol medium and 15 OD of cells were used for glass beads extraction and 1.5 OD for TCA extraction. Cells for glass beads extraction were pelleted and resuspended in 200 ul of phosphate-buffered saline (PBS) containing 50 mM NaF (NaF was used to deactivate endogenous phosphatase), 0.5% wt/vol SDS, and 1% vol/vol β-mercaptoethanol. Cell debris was removed by centrifugation for 1 min at 8000 g. The supernatant was boiled for 5 min. 100 ul of cell-free lysate was added to 400 ul of buffer containing 50 mM MES pH 6.0, 1 mM DTT and protease inhibitors (1 mM PMSF, 1 mM protease inhibitor cocktail, 1 mM leupeptin, and 1 mM aprotinin). Samples were incubated for 2 h at 30°C. Mock controls were treated in a similar manner, but without the addition of NaF. All samples were TCA precipitated (2) and boiled for 5 min prior to SDS-PAGE and western blotting (1).

PAP treatment in presence of NaF

Cells from grown for 4 h in methanol medium and 10 OD of cells were pelleted and resuspended in 200 ul of immunoprecipitation (IP) buffer containing 0.5% vol/vol NP40, 50 mM HEPES-KOH pH 7.4, 500 mM NaCl, 1 mM EDTA, 10% vol/vol glycerol, 50 mM NaF and protease inhibitors (1 mM PMSF, 1 mM protease inhibitor cocktail, 1 mM leupeptin, and 1 mM aprotinin). Cell debris was removed by centrifugation at 21000

g for 10 min. 40 ul of 6x SDS loading buffer was added to supernatant and boiled for 5 min. 10 ul of this loading sample was used for PAP treatment as described above.

Large scale affinity purification of Rppa09976-HA

Cells were grown for 4 h in methanol medium. 1500 OD of cells were pelleted and resuspended in 10 ml of IP buffer containing 0.5% vol/vol NP40, 50 mM HEPES-KOH pH 7.4, 500 mM NaCl, 1 mM EDTA, 10% vol/vol glycerol, 50 mM NaF and protease inhiditors (1 mM PMSF, 1 mM protease inhibitor cocktail, 1 mM leupeptin, and 1 mM aprotinin). From this step, everything was done in a keratin free environment. Cell debris was removed by centrifugation at 21000 g for 10 min. 40 ul was taken as lysate sample. The cell lysate was incubated 4 h at 4°C with 300 ul of washed EZview™ Red Anti-HA Affinity Gel (Sigma), to bind Rppa09976-HA. 40 ul was taken as unbound sample, for loading on SDS-PAGE. Anti-HA Affinity Gel was washed three times with IP buffer. Rppa09976-HA bound to the anti-HA beads was eluted sequentially twice with 300 ul of 0.1 M glycine-HCl pH 2.5 and once with 300 ul of 0.1 M glycine + 8 M urea pH 3.3, all three elutions were neutralized with 2M Tris base. The remaining protein was eluted with 300 ul of 1% wt/vol SDS. 40 ul of Lysate, the unbound fraction and all elutions were mixed separately with 8 ul of 6X SDS loading buffer and boiled for 5 min prior to SDS-PAGE western blotting (1) and silver staining (Invitrogen).

Mass Spectrometry

First glycine eluate from the large scale purification of Rppa09976-HA was treated with trypsin. The peptide mixture was subjected to immobilized metal affinity

chromatography (IMAC) in order to enrich for phosphopetides. The peptide fragments identified by mass spectrometry were matched to the amino acid sequence of Rppa09976. Phosphorylated residues were found and marked (mass spectrometry done in Dr. H. Zhou's lab, UCSD Department of Cell & Molecular Medicine).

Results

A. Previous findings of our lab on Rppa09976

Rppa09976 was found by mass spectrometry analysis as a putative interacting partner of TAP-tagged Pex3, a peroxisomal membrane protein required for peroxisome biogenesis. Rppa09976 encodes a 44 kDa protein containing an N-terminal acyl-CoA binding domain (ACBD) including a conserved acyl-CoA binding site, two transmembrane domains and three potential Atg8 binding motifs (Figure 2-1). Rppa09976 is a pexophagy specific protein that is expressed during methanol adaptation. It accumulates its first modification (as judged by slower migrating bands upon SDS-PAGE) after 2 h in methanol medium which coincides with its localization on peroxisomes. At latter time points an additional modified species of Rppa09976 appears (Figure 2-2) (3).

B. Rppa09976 is a phosphoprotein

i. PAP dephosphorylates Rppa09976 in cell lysates prepared by glass beads

To find the nature of multiple modified forms of Rppa09976, we chose the 4 h time point because Rppa09976 already contains both modifications at a relatively high amount. Our initial hypothesis was that it is phosphorylation. We used Pex14 as a

positive control because it was shown to be a highly phosphorylated protein (4). To test this, we used PAP (Potato acid phosphatase) and CIP (Calf Intestinal Alkaline Phosphatase), two commonly used phosphatases that remove phosphate groups nonspecifically. TCA extracts of Rppa09976 were used for phosphatase treatment. Using the recommended amounts of protein, enzyme and incubation time did not provide any alteration of the modified, slower-migrating bands during SDS-PAGE. Atg30, the receptor for pexophagy is a confirmed phosphoprotein which was dephosphorylated previously in our lab with PAP in cell lysates prepared by post-alkaline extraction. Replicating this protocol was unsuccessful at depleting modified forms of Rppa09976. Some modified forms of Rppa09976 were also sensitive to alkaline conditions as they were less abundant compared to the lysate prepared by TCA extraction. Next, we tried the glass beads extraction and treated the lysate with PAP based on a protocol described earlier (4). This method showed depletion of the modifications of both Rppa09976 and Pex14 in samples treated with PAP (Figure 2-3), suggesting that Rppa09976 is a phosphoprotein.

ii. NaF in lysis buffer prevents dephosphorylation of Rppa09976 by endogenous phosphatases

Glass bead extraction of proteins from yeast cells leads to a lower amount of highest molecular weight form of Rppa09976 compared to that obtained from a TCA extract. This could be due to the presence of endogenous phosphatases, which are inactivated by TCA, but stay active in the glass bead lysate. In addition, in the glass bead lysate, modified bands are fuzzy and it is not clear which bands of the TCA lysate they correspond to. To clarify these uncertainties, samples prepared by TCA and glass bead

extractions were run in parallel. NaF was used to inhibit endogenous phophatases in the glass bead sample. In the presence of NaF (+), there were two modified bands of Rppa09976 which are equivalent in molecular weight to those found in the TCA lysates. Glass bead lysates prepared in the absence of NaF (-) mostly showed one modified band - the highest molecular weight modification of Rppa09976 that is present in NaF (+) and TCA lysates was missing (Figure 2-4).

iii. PAP completely dephosphorylates all modified forms of Rppa09976 preserved by NaF

In order to show directly that all modified forms of Rppa09976 can be removed by PAP and hence they are phosphorylated forms, we aimed to treat samples prepared in presence of NaF with PAP. Although one might question this strategy as NaF would possibly deactivate PAP, we showed that this assay is the best way to dephosphorylate Rppa09976. Samples prepared in IP buffer containing NaF showed clear modified bands of Rppa09976 and all of them collapsed to the lowest molecular weight form upon treatment with PAP (Figure 2-5). As shown in Figure 2-4, this band is equivalent to the lowest molecular band of samples prepared with TCA. Therefore, we argue that all modified forms of Rppa09976 are phosphorylated bands.

C. Prediction of Phosphorylation sites of Rppa09976

After finding that Rppa09976 is phosphorylated, it was necessary to find the phosphorylated residues. Before proceeding with protein purification and subsequent mass spectrometry analysis, we used PROSITE software to check potential phosphorylation sites. This software revealed 11 protein kinase C (PKC) sites, 11 casein

kinase II (CK2) sites and 1 cAMP/cGMP dependent protein kinase phosphorylation sites. In total there are 23 potential non-overlapping phosphorylation sites (Figure 2-6).

D. Mass spectrometry reveals multiple phosphosites

i. Affinity purification of Rppa09976-HA using Anti-HA Affinity Gel

We affinity purified Rppa09976-HA for mass spectrometry analysis. As in dephosphorylation experiments, the cells induced in methanol medium for 4 h were used, which contain all modified forms of Rppa09976. Most of the protein was bound to the Anti-HA Affinity Gel and stayed bound to the beads during washing. A large fraction of Rppa09976-HA was released from the beads by the first glycine elution and the remaining protein was released in subsequent elutions (Figure 2-7). The purity of the first elution was confirmed with silver staining of SDS-PAGE gel and was subjected to IMAC analysis.

ii. Analysis of Rppa09976 phosphorylation profile

Affinity purified Rppa09976-HA subjected to IMAC mass spectrometry revealed multiple phosphopeptides and phosphorylated sites. Phosphopeptides covered 62 % of the protein amino acid sequence. Phosphopeptide fragments contained 21 phosphorylated residues. Amongst phosphorylated residues, 10 predicted were found. There were 6 residues that were predicted to be phosphorylated but not confirmed by IMAC and 7 predictions were assigned to the fragments not covered by Phosphopeptides (Figure 2-8).

Discussion

Phosphorylation of Rppa09976 correlates with its peroxisomal localization as both events coincide temporally. Since Rppa09976 and Atg30 interact and colocalize on peroxisomal membrane, they both may be phosphorylated by the same kinase. Atg30 phosphorylation is Pex3 dependent, which means that like Rppa09976, Atg30 might be phosphorylated by a peroxisomal membrane kinase. However, the Atg30 and Rppa09976 kinase/s remain unidentified at present. PROSITE software predicted that PKC, CK2 or a cAMP/cGMP-dependent kinase might be responsible for phosphorylation of Rppa09976. It is unclear if Rppa09976 phosphorylation is of functional significance for pexophagy as it happens during peroxisomal induction conditions, but the protein has a role in peroxisome degradation, whereas Atg30 phosphorylation happens after induction of pexophagy and is required for pexophagy. It will be of particular interest to test whether or not the observed phosphorylation is important for pexophagy. However, many phosphorylated residues were found in mass spectrometry results, so it may be vastly time consuming to find a phosphorylation site mutant that is blocked in pexophagy, which is beyond the scope of this thesis.

Chapter 2 is currently being prepared to submit for publication of the material. Lotfi, Pouya; Ozeki, Katharine; Nazarko, Taras Y; and Subramani, Suresh. The thesis author was the primary investigator and author of this paper.

Table 2-1. *P. pastoris* strains and plasmids used in this study.

Name	Genotype and plasmid	Source
PPY12h	arg4 his4	(Gould et al., 1992)
STN96	PPY12h Δ*rppa09976*::Geneticin^{R} (pMY92K)	Subramani Lab
STN128	STN96 *his4*::pMY323 ($P_{RPPA09976}$-RPPA09976-GFP, HIS4)	Subramani Lab
STN151	STN128 *arg4*::pJCF402 (P_{GAPDH}-BFP-SKL, ARG4)	Subramani Lab
STN215	STN96 *his4*::pMY320 ($P_{RPPA09976}$-RPPA09976-HA, HIS4)	This study
STN290	STN96 *his4*::pTYN19 ($P_{RPPA09976}$-RPPA09976-HA, W119A, I122A)	This study
STN292	STN96 *his4*::pTYN21 ($P_{RPPA09976}$-RPPA09976-HA, Y40F, K44A, HIS4)	This study
STN294	STN96 *his4*::pTYN24 ($P_{RPPA09976}$-RPPA09976-GFP, ΔTMD, HIS4)	This study
STN295	STN96 *his4*::pTYN24 ($P_{RPPA09976}$-RPPA09976-GFP, ΔTMD, HIS4)	This study
STN296	STN96 *his4*::pTYN24 ($P_{RPPA09976}$-RPPA09976-HA, ΔTMD, HIS4)	This study
STN298	STN96 *his4*::pTYN20 ($P_{RPPA09976}$-RPPA09976-GFP, W119A,I122A, HIS4)	This study
STN299	STN96 *his4*::pTYN20 ($P_{RPPA09976}$-RPPA09976-GFP, W119A,I122A, HIS4)	This study
STN300	STN96 *his4*::pTYN22 ($P_{RPPA09976}$-RPPA09976-GFP, Y40F, K44A, HIS4)	This study
STN301	STN96 *his4*::pTYN22 ($P_{RPPA09976}$-RPPA09976-GFP, Y40F, K44A, HIS4)	This study
STN362	STN96 *arg4*::pJCF477 (P_{ATG8}-mCherry-ATG8, ARG4)	This study
STN363	STN215 *arg4*::pJCF477 (P_{ATG8}-mCherry-ATG8, ARG4)	This study
STN365	STN290 arg4::pJCF477 (P_{ATG8}-mCherry-ATG8, ARG4)	This study
STN415	SJCF755::pKO4 ($P_{RPPA09976}$-RPPA09976-HA, Hygromycin^{R})	This study
STN420	STN362 *his4*::pTYN28 ($P_{RPPA09976}$-RPPA09976-HA, Y25A, L28A, W119A, I122A, HIS4)	This study
STN424	STN362 *his4*::pTYN30 ($P_{RPPA09976}$-RPPA09976-HA, W119A, I122A, Y40F, K44A, HIS4)	This study
STN426	STN362 *his4*::pTYN27 ($P_{RPPA09976}$-RPPA09976-HA, Y25A, L28A, HIS4)	This study
SJCF755	Δ*atg26 his4*::pJCF45 (P_{GAPDH}-ATG30-GFP, HIS4)	Subramani Lab

MSESIDRVFV KAIGTIRTLS SRTGYGGLPR PPIENRVKLY GLYKQATEGD
VAGVMERPLG DSPEAEAAKR KWDAWRSEQG TSKTEAKRQY ISYLIDTMKQ
FASDTTEARE LLSELEYLWN QISDVSPNDS SDSESNAGPA QLLQNHAQLL
SRDISVVDDP ITSSGMDPMY NPSFQRHNSS RFINASTAER LNSLSNYYSN
LNPTPPLSSR RYQGSVTPRN VDFIKWQNDI NNSINKLNHD LQLLANRRLQ
SSASDPLYSK RGSDLTHDDF VNDISSSSSN RRFRARRNQP LVSKVLLGTI
SLLLKLIKTV IKHVAIDAVI IAVLVAVIKR SIIIPNLISN EISLQKIHHS
ELESNSSIKG DSNGGRLTIV LPFINGKDFF QENSLLGKLL KVFHDYVDHV
SRIRLIKRN

Figure 2-1: Functional domains and motifs of Rppa09976, acyl-CoA binding domain, two transmembrane domains, putative Atg8 binding sites (LIR motif), conserved acyl-CoA binding site.

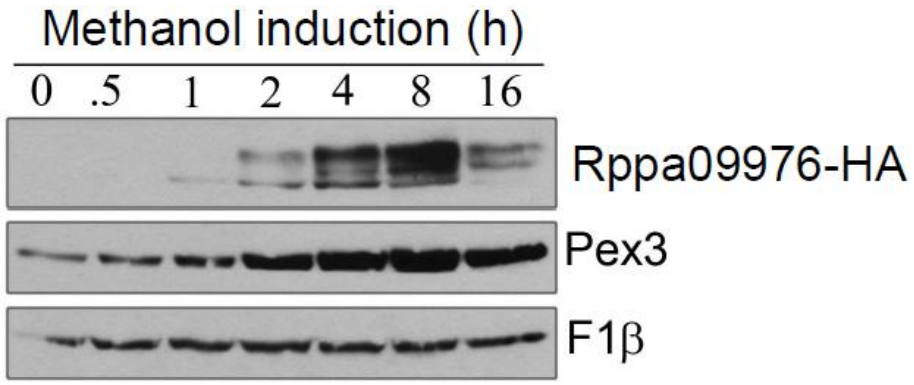

Figure 2-2: Rppa09976 modification. *Δrppa09976* cells expressing Rppa09976-HA (STN215) were induced in methanol medium for number of hours indicated.

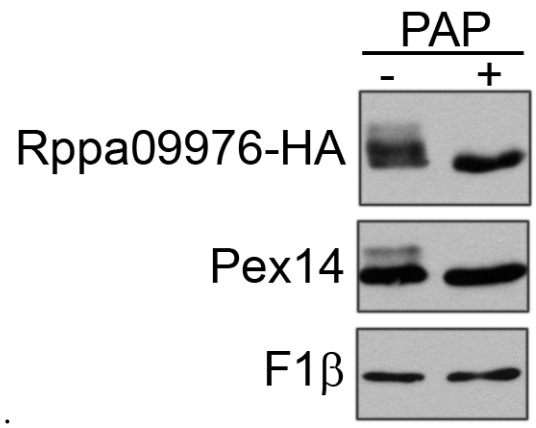

Figure 2-3: PAP dephosphorylates Rpp09976-HA in cell lysates prepared by glass beads. *Δrppa09976* cells expressing Rppa09976-HA (STN215) were induced 4 h in methanol medium. 0.3 OD of cells was incubated for 2 h with (+) and without (-) PAP at 30°C.

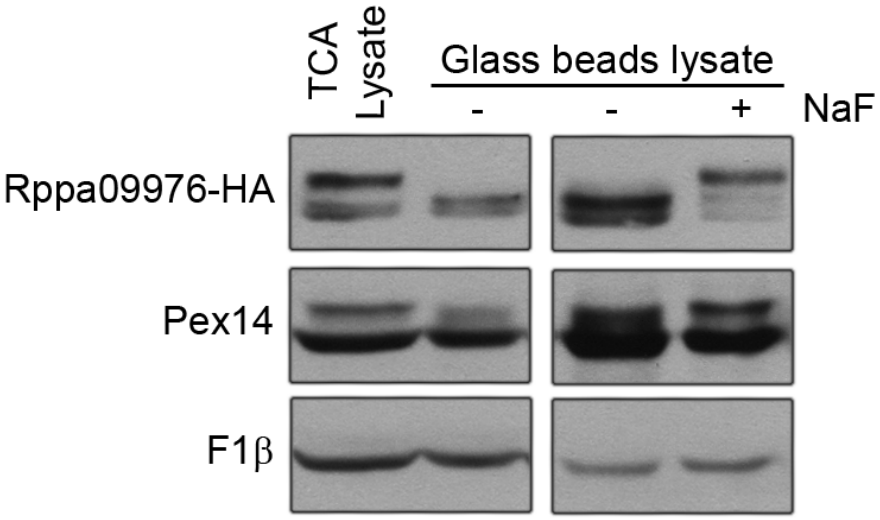

Figure 2-4: NaF preserves the higher molecular weight, phosphorylated bands of Rppa09976-HA and Pex14 in glass bead lysates. *Δrppa09976* cells expressing Rppa09976-HA (STN215) cells were induced 4 h in methanol medium. 1.5 OD of cells were prepared by TCA extraction. 7.5 OD of cells were prepared by glass beads extraction and incubated for 2 h with (+) and without (-) 50 mM NaF at 30°C.

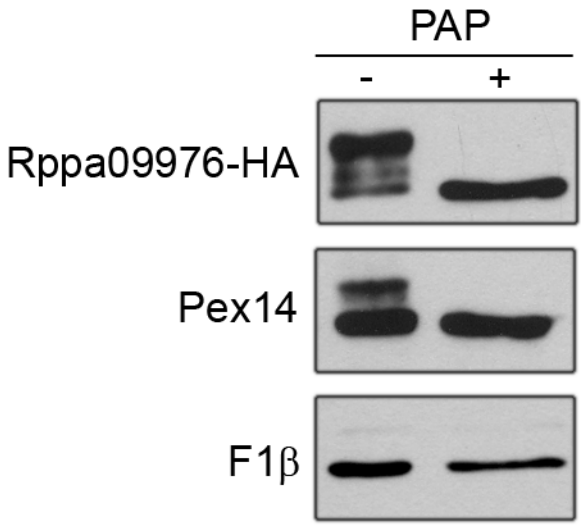

Figure 2-5: PAP completely removes all modified forms of Rppa09776 preserved by NaF. *Δrppa09976* cells expressing Rppa09976-HA (STN215) cells were induced for 4 h in methanol medium. Cell lysates were prepared with 1% Triton-X100 in the presence of NaF. 0.4 OD of cells were incubated for 2 h with (+) and without (-) PAP at 30°C.

MSESIDRVFV KAIGTIRTLS SRTGYGGLPR PPIENRVKLY GLYKQATEGD
VAGVMERPLG DSPEAEAAKR KWDAWRSEQG TSKTEAKRQY ISYLIDTMKQ
FASDTTEARE LLSELEYLWN QISDVSPNDS SDSESNAGPA QLLQNHAQLL
SRDISVVDDP ITSSGMDPMY NPSFQRHNSS RFINASTAER LNSLSNYYSN
LNPTPPLSSR RYQGSVTPRN VDFIKWQNDI NNSINKLNHD LQLLANRRLQ
SSASDPLYSK RGSDLTHDDF VNDISSSSSN RRFRARRNQP LVSKVLLGTI
SLLLKLIKTV IKHVAIDAVI IAVLVAVIKR SIIIPNLISN EISLQKIHHS
ELESNSSIKG DSNGGRLTIV LPFINGKDFF QENSLLGKLL KVFHDYVDHV
SRIRLIKRN

Figure 2-6: Predicted phosphorylation sites of Rppa09976. Phosphosites predicted by PROSITE are underlined, 23 predicted phosphorylated residues, acyl-CoA binding domain, two transmembrane domains.

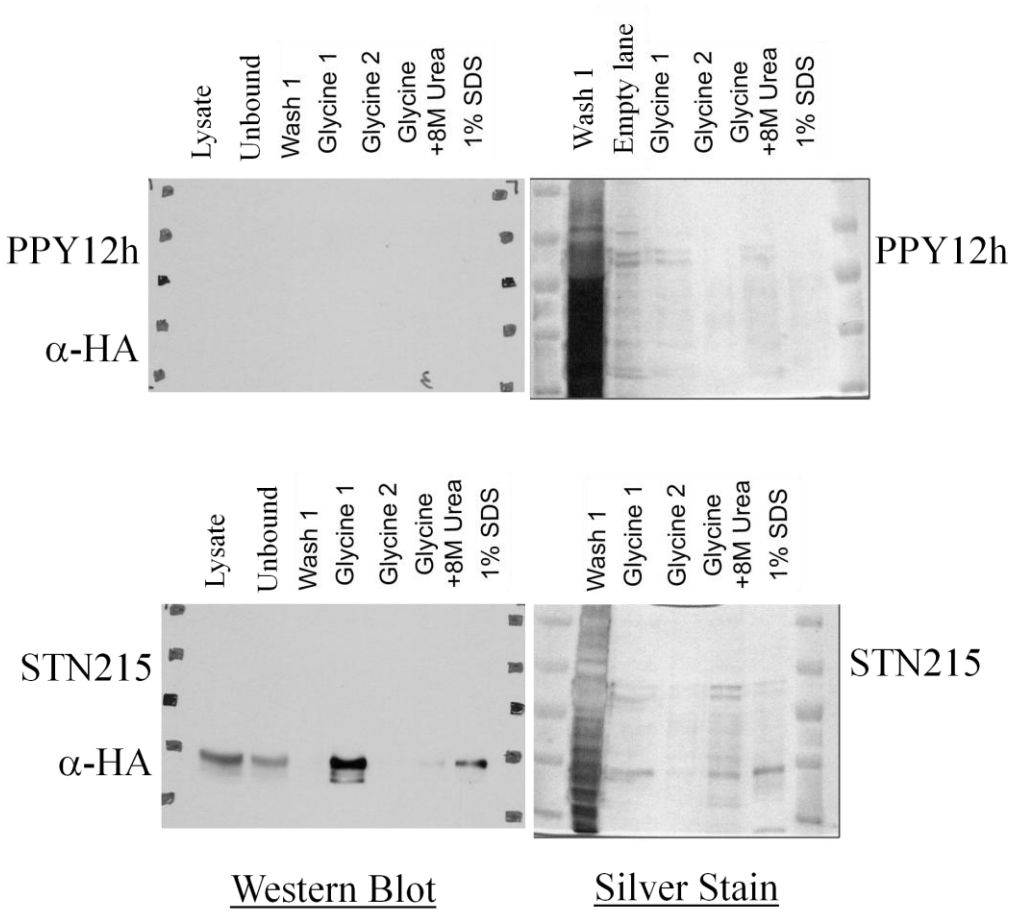

Figure 2-7: Large scale affinity purification of Rppa09976-HA. PPY12h and *Δrppa09976* cells expressing Rppa09976-HA (STN215) cells were induced for 4 h in methanol medium. 1500 OD of cells were used to prepare the Lysate, which was incubated with Anti-HA Affinity Gel. First glycine elution was subjected to IMAC mass spectrometry for mapping of phosphorylation sites.

MSESIDRVFV KAIGTIRTLS SR**TGYGGLPR PPIENRVKLY GLYKQATEGD**
VAGVMERPLG DSPEAEAAKR KWDAWRSEQG TSKTEAK**RQY ISYLIDTMKQ**
FASDTTEARE LLSELEYLWN QISDVSPNDS SDSESNAGPA QLLQNHAQLL
SR**DISVVDDP ITSSGMDPMY NPSFQRHNSS RFINASTAER LNSLSNYYSN**
LNPTPPLSSR RYQGSVTPRN VDFIK**WQNDI NNSINKLNHD LQLLANRRLQ**
SSASDPLYSK RGSDLTHDDF VNDISSSSSN RRFRARRNQP LVSKVLLGTI
SLLLKLIKTV IKHVAIDAVI IAVLVAVIKR SIIIPNLISN EISLQ**KIHHS**
ELESNSSIKG DSNGGRLTIV LPFINGKDFF QENSLLGKLL K**VFHDYVDHV**
SRIRLIKRN

Figure 2-8: Predicted and found phosphorylation sites of Rppa09976. Phosphosites predicted by PROSITE are underlined. Phosphopeptides found by IMAC mass spectrometry are in bold, found phosphorylated residues, phosphopeptides predicted but not covered in mass spec, acyl-CoA binding domain, two transmembrane domains.

References

1. Laemmli, U. K. (1970) Cleavage of structural proteins during the assembly of the head of bacteriophage T4, *Nature 227*, 680-685.

2. Baerends, R. J., Faber, K. N., Kram, A. M., Kiel, J. A., van der Klei, I. J., and Veenhuis, M. (2000) A stretch of positively charged amino acids at the N terminus of Hansenula polymorpha Pex3p is involved in incorporation of the protein into the peroxisomal membrane, *J Biol Chem 275*, 9986-9995.

3. Ozeki, K. (2009) Pichia pastoris Rppa09976 is a peroxisomal membrane-associated ACBP domain-containing protein, deliverd to peroxisomes from the ER, and is required for their selective degradation., In *Biology*, University of California, San Diego.

4. Johnson, M. A., Snyder, W. B., Cereghino, J. L., Veenhuis, M., Subramani, S., and Cregg, J. M. (2001) Pichia pastoris Pex14p, a phosphorylated peroxisomal membrane protein, is part of a PTS-receptor docking complex and interacts with many peroxins, *Yeast 18*, 621-641.

Chapter III: Rppa09976 interactions

Strains

Pichia pastoris strains used in this study are described in Table 2-1.

Micropexophagy induction

P. pastoris cells were pre-grown to the late exponential-stationary phase in YPD medium, diluted 25 fold in fresh YPD medium and pre-grown to the early-mid exponential phase again in YPD medium. Cells were washed twice with YNB solution and transferred to peroxisome-induction medium at an OD_{600} of 0.3 for 15 h. Cells were washed with YNB solution and inoculated into micropexophagy-induction medium (1.7 g/l YNB without amino acids, 2% wt/vol glucose and 0.5% wt/vol ammonium sulfate). Histidine (50 mg/l) and/or arginine (50 mg/l) was added, when needed.

Rppa09976-HA immunoprecipitation

150 OD of P. pastoris cells induced in peroxisome biogenesis conditions or micropexophagy conditions were pelleted and resuspended in 1ml of IP buffer containing 0.5% vol/vol NP40, 50 mM HEPES-KOH pH 7.4, 50 mM NaCl, 1 mM EDTA, 10% vol/vol glycerol, 10 mM NaF and protease inhibitors (1 mM PMSF, 1mM protease inhibitor cocktail, 1mM leupeptin, and 1mM aprotinin). Cell debris was removed by centrifugation at 21000 g for 10 min. 25 ul was taken as input sample and diluted eight times and mixed with 40 ul of 6X SDS loading buffer and boiled for 5 min. The cell lysate was incubated 4 h at 4°C with 50 ul of washed EZview™ Red Anti-HA Affinity

Gel (Sigma), to bind Rppa09976-HA. Anti-HA Affinity Gel bound to Rppa09976-HA was washed three times with IP buffer. Rppa09976-HA was eluted from the Anti-HA Affinity Gel with 200 ul of 0.1 M glycine-HCl, pH 2.5 and was immediately neutralized with 2M Tris base. Input and elution fractions (IP Rppa09976-HA) were mixed with 40 ul of 6X SDS loading buffer and boiled for 5 min prior to SDS-PAGE and western blotting (1). Each lane was loaded with 15 ul sample, as follows: Input 0.3 OD equivalent and IP Rppa09976-HA 11.2 OD equivalent.

mCherry-Atg8 Immunoprecipitation

25 OD of cells induced in micropexophagy conditions were pelleted and resuspended in 250 ul of IP buffer containing 0.5% vol/vol NP40, 50 mM HEPES-KOH pH 7.4, 50 mM NaCl, 1 mM EDTA, 10% vol/vol glycerol, 10 mM NaF and protease inhibitors (1 mM PMSF, 1mM protease inhibitor cocktail, 1 mM leupeptin, and 1 mM aprotinin). Cell debris was removed by centrifugation at 21000 g for 10 min. The cell lysate was incubated 1 h at 4°C with 50 ul of washed GammaBind G Sepharose (GE), to pre-clear the lysate of proteins that bind Sepharose nonspecifically. 10 ul of pre-cleared lysate was taken as input and diluted 20 times, and mixed with 200 ul of 2X SDS loading buffer and boiled for 5 min. The remaining 240 ul of pre-cleared lysate was incubated overnight at 4°C with 10 ul of DsRed polyclonal antibody (Living Colors). In order to pull-down mCherry-Atg8 bound to antibody, 50 ul of washed GammaBind G Sepharose was added to the lysate and incubated 1 h at 4°C. GammaBind G Sepharose was washed three times with IP buffer. Bound mCherry-Atg8 was eluted with 50 ul of 2X SDS loading buffer and boiled for 5 min prior to SDS-PAGE and western blotting (1). Each

lane was loaded with 20 ul sample, as follows: Input 0.05 OD equivalent and IP mCherry-Atg8 9.6 OD equivalent.

Atg30-GFP immunoprecipitation

25 OD of cells induced in micropexophagy conditions were pelleted and resuspended in 250 ul of IP buffer containing 1% wt/vol CHAPS, 50 mM HEPES-KOH, pH 7.4, 150 mM NaCl, 1 mM EDTA, 10% vol/vol glycerol, 50 mM NaF and protease inhibitors (1 mM PMSF, 1 mM protease inhibitor cocktail, 1 mM leupeptin, and 1 mM aprotinin). Cell debris was removed by centrifugation at 500 x g for 10 min. The membrane protein solubiliztion was perfomed by incubation of the lysate at 4°C for 1 h with rotation and was then centrifuged at 21000 g for 10 min. The cell lysate was incubated 1 h at 4°C with 50 ul of washed GammaBind G Sepharose, to pre-clear the lysate of proteins that bind Sepharose nonspecifically. 20 ul of pre-cleared lysate was taken as input and mixed with 4 ul of 6X SDS loading buffer and boiled for 5 min. The remaining 230 ul of pre-cleared lysate was incubated overnight at 4°C with 10 ul of Atg30 polyclonal antibody (made in our lab). In order to pull-down Atg30-GFP bound to antibody, 50 ul of washed GammaBind G Sepharose was added to lysate and incubated 1 h at 4°C. GammaBind G Sepharose was washed three times with IP buffer. Bound Atg30-GFP was eluted with 30 ul of 2X SDS loading buffer and boiled for 5 min prior to SDS-PAGE and western blotting (1). Each lane was loaded with 20 ul sample, as follows: Input 2 OD equivalent and IP Atg30-GFP 15.3 OD equivalent.

Results

A. Rppa09976-HA interacts with Pex3 under peroxisome-biogenesis and micropexophagy conditions

Rppa09976 was found by mass spectrometry analysis as a putative interacting partner of TAP-tagged Pex3, a peroxisomal membrane protein required for peroxisome-biogenesis. Functional Rppa09976-HA was immunoprecipitated to confirm this interaction and to look for possible interactions with other peroxisomal membrane proteins. Western blot of immunoprecipitated Rppa009976-HA showed co-immunoprecipitated Pex3 (Figure 3-1), a core peroxisomal membrane protein that is delivered to peroxisomes at the earliest stages of peroxisomal biogenesis (2). Pex3 co-immunoprecipitation was absent in the strain without Rppa09976-HA indicating that Pex3 is co-immunoprecipitated with Rppa09976-HA and does not bind to the Anti-HA Affinity Gel, nonspecifically. We also checked Rppa09976-HA interaction with Pex19, which is responsible for delivery and localization of peroxisomal membrane proteins (2), however the results were negative. Rppa09976-HA does not seem to interact with other peroxisomal membrane proteins that are involved in peroxisomal matrix protein delivery such as Pex8, Pex13, Pex14, Pex17, Pex2, Pex10 and Pex12 (Figure 3-1). AOX, a peroxisomal matrix protein, was used as a negative control. We also checked interaction of Rppa09976-HA with Pex3 under micropexophagy conditions. As under peroxisome biogenesis conditions, during micropexophagy Rppa09976-HA interacted with Pex3 but not with other peroxisomal membrane proteins (Figure 3-2).

B. Rppa09976-HA interacts with mCherry-Atg8 and Atg30-GFP under micropexophagy conditions

The pexophagy receptor, Atg30, is known to interact with Atg11 and Atg17, localized at the PAS (3). However, unlike other selective autophagy receptors, Atg30 does not interact with Atg8, which is localized on growing isolation membranes. In order to find interacting partners of Rppa09976 amongst Atg proteins we picked the most probable candidates: Atg8, Atg11, Atg17 and Atg30 and used tagged Atg proteins because we did not have antibody against Atg proteins. We immunoprecipitated mCherry-Atg8 under micropexophagy conditions and looked for co-immunoprecipitated Rppa09976-HA. This showed interaction of Atg8 and Rppa09976 (Figure 3-3) only in the strain expressing Rppa09976-HA.

Detecting the interactions of Rppa09976 with Atg30 is complicated by the low expression level of Atg30 because of its strong membrane association and its degradation when pexophagy is induced (3). To avoid these problems, we immunoprecipitated overexpressed Atg30-GFP in the Δ*atg26* strain to block pexophagy and to enrich for possible interactions. Immunoprecipitated Atg30-GFP showed co-immunoprecipitated Rppa09976-HA (Figure 3-4), only in the strain expressing Rppa09976-HA. We also checked the interaction of Rppa09976 with Atg11 and Atg17, both of which interact with Atg30, but we could not observe co-immoprecipitation of Rppa09976-HA with these proteins (data not shown).

Discussion

Selective autophagy is accomplished through a conserved theme where cargo is recognized by receptor proteins that interact with the autophagy proteins, Atg8 and Atg11. In the case of the Cvt and mitophagy pathways, Atg19 and Atg32 are the

receptors, linking the Ape1 complex and mitochondria, respectively, to the expanding isolation membrane and autophagy machinery by interacting with Atg8 and Atg11, respectively. In pexophagy, Atg30 tags peroxisomes for degradation by interacting with peroxisomal membrane proteins, Pex3 and Pex14, and autophagy machinery proteins, Atg11 and Atg17; however, the link to Atg8 is undetectable. Interestingly, these missing links are provided via Rppa09976, which interacts with Pex3, Atg8 and Atg30. We propose a model where Rppa09976 acts as the co-receptor for pexophagy and bridges peroxisomes and Atg30 to the growing isolation membrane (Figure 3-5). Unlike other selective autophagy types; pexophagy requires an extra receptor protein for sequestering peroxisomes. In *P. pastoris*, pexophagy is triggered by specific carbon sources, which is different from those necessary for the Cvt and mitophagy pathways, which occurs independent of carbon source in basal conditions. Perhaps, the need of co-receptors in pexophagy evolved to adapt for sequestration of cargo by autophagy machinery after switch of carbon source from methanol, a non-basal condition. Methanol adaptation leads to the formation of a cluster of giant peroxisomes, whereas oleate adaption leads to the formation of smaller, individual peroxisomes. It has been shown that larger peroxisomes require more specific autophagic machinery proteins (4). This might explain why Atg30 and Rppa09976 homologues are missing in *Saccharomyces cerevisiae* where peroxisomes are only induced under oleate adaptation. As a test of this hypothesis, we predict that Rppa09976 might not be required for degradation of small oleate-induced peroxisomes in *P. pastoris*.

Chapter 3 is currently being prepared to submit for publication of the material. Lotfi, Pouya; Ozeki, Katharine; Nazarko, Taras Y; and Subramani, Suresh. The thesis author was the primary investigator and author of this paper.

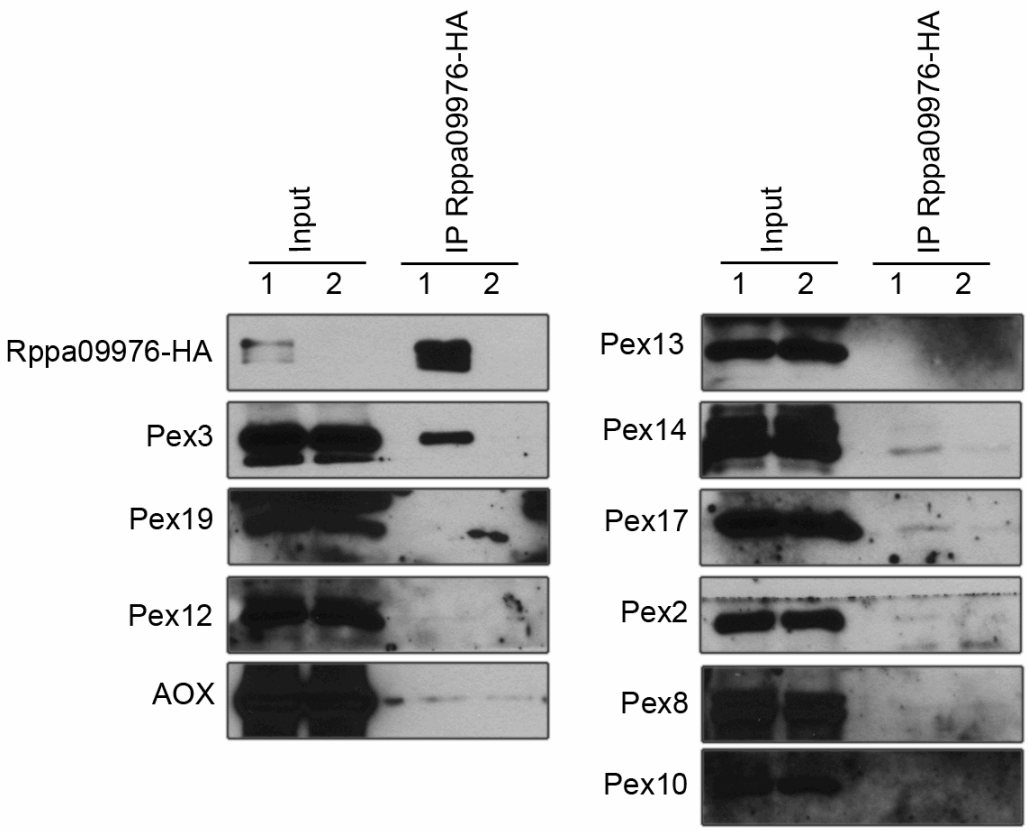

Figure 3-1: Co-immunoprecipitation of Rppa09976-HA and Pex3 during methanol adaptation. WT (lane 2, PPY12h) and Δ*rppa09976* cells expressing Rppa09976-HA (lane 1, STN215) were induced for 4 h in methanol medium. Immunoprecipitation was performed as described in Materials and Methods.

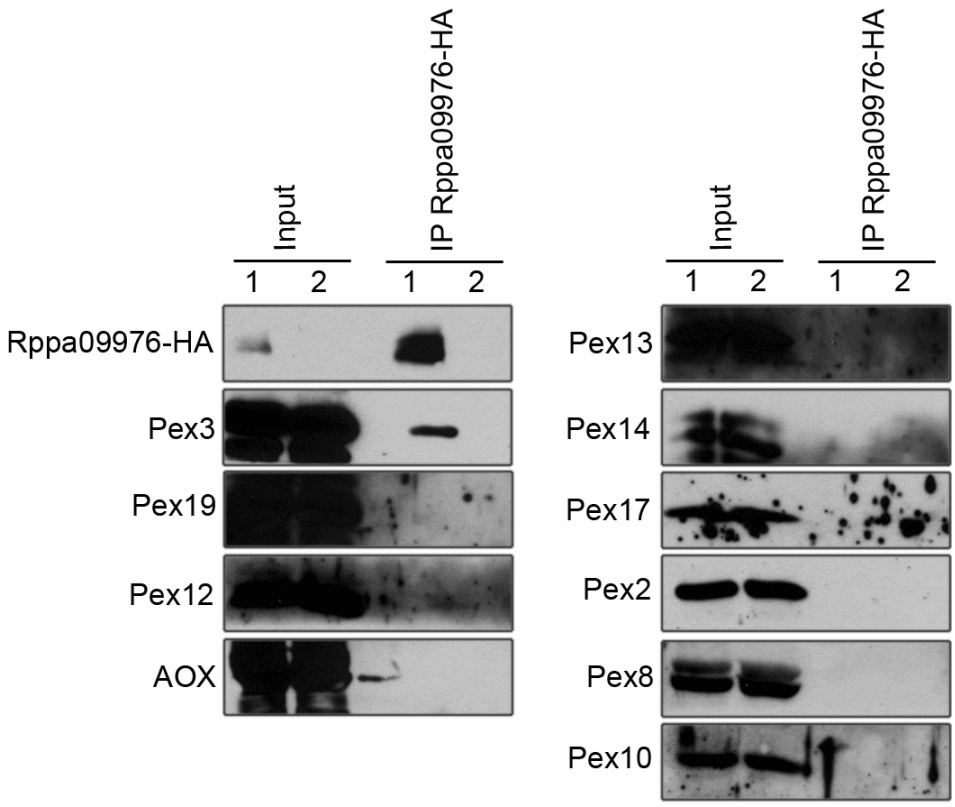

Figure 3-2: Co-immunoprecipitation of Pex3 with Rppa09976-HA under micropexophagy conditions. WT (lane 2, PPY12h) and Δ*rppa09976* cells expressing Rppa09976-HA (lane 1, STN215) were induced for 16 h in methanol medium and transferred for 0.5 h to glucose medium. Immunoprecipitation was performed as described in Materials and Methods.

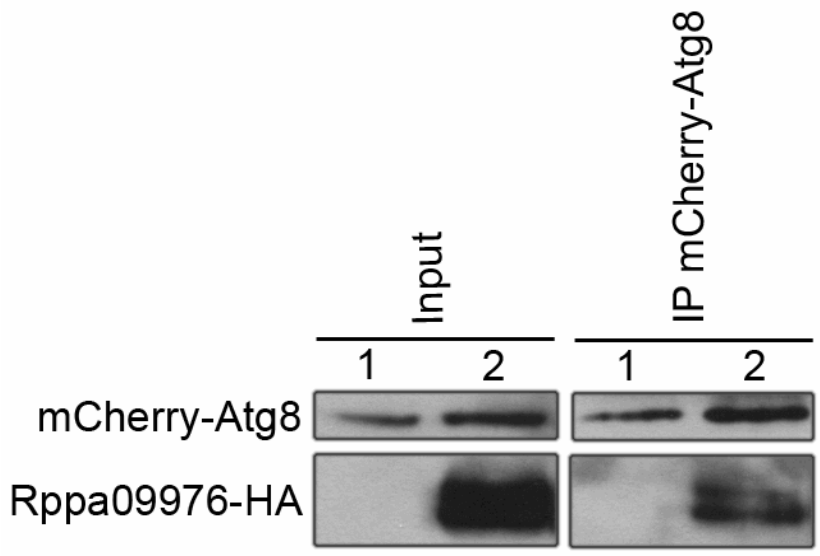

Figure 3-3: Rppa09976-HA co-immunoprecipitated with mCherry-Atg8 under micropexophagy conditions. Δ*rppa09976* cells (lane 1, STN362) and Δ*rppa09976* cells expressing Rppa09976-HA (lane 2, STN363) were induced for 16 h in methanol medium and transferred for 0.5 h to glucose medium. Both strains expressed mCherry-Atg8. Immunoprecipitation was performed as described in Materials and Methods.

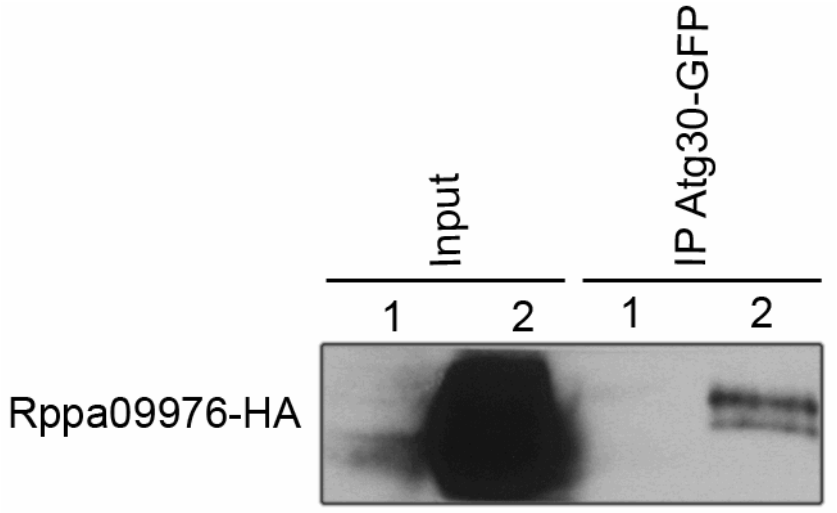

Figure 3-4: Rppa09976-HA co-immunoprecipitated with Atg30-GFP under micropexophagy conditions. Δ*atg26* cells (lane 1, SJCF755) and Δ*atg26* cells expressing Rppa09976-HA (lane 2, STN415) were induced for 16 h in methanol medium and transferred for 0.5 h to glucose medium. Both strains expressed Atg30-GFP. Immunoprecipitation was performed as described in Materials and Methods.

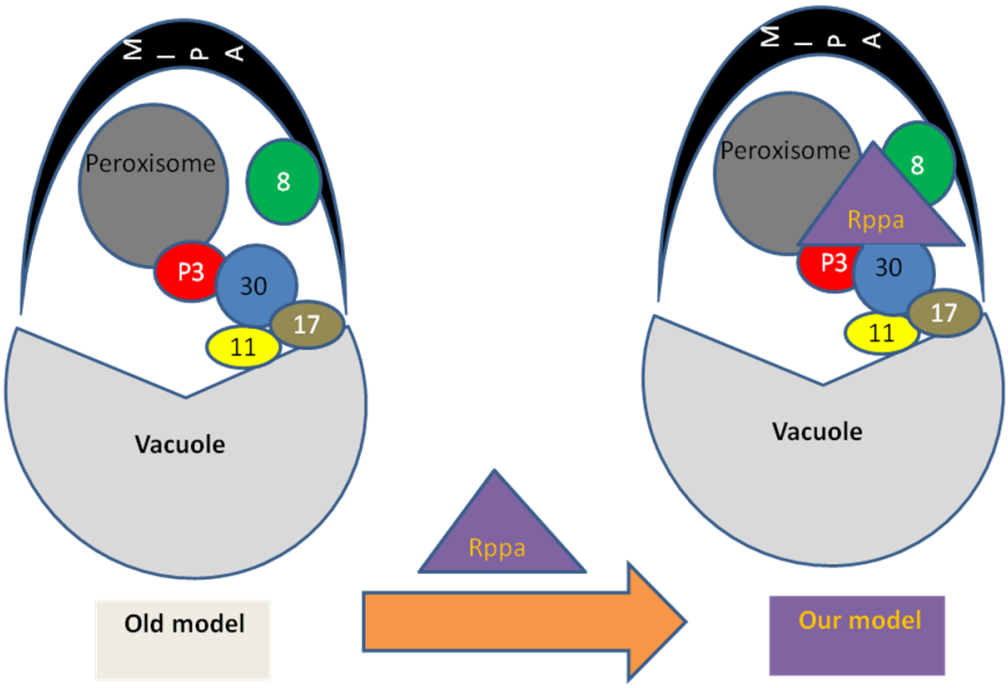

Figure 3-5: Rppa09976 interacts with Pex3, Atg8 and Atg30, perhaps guiding the growing MIPA around peroxisomes tagged for degradation.

References

1. Laemmli, U. K. (1970) Cleavage of structural proteins during the assembly of the head of bacteriophage T4, *Nature 227*, 680-685.

2. Snyder, W. B., Koller, A., Choy, A. J., and Subramani, S. (2000) The peroxin Pex19p interacts with multiple, integral membrane proteins at the peroxisomal membrane, *J Cell Biol 149*, 1171-1178.

3. Farre, J. C., Manjithaya, R., Mathewson, R. D., and Subramani, S. (2008) PpAtg30 tags peroxisomes for turnover by selective autophagy, *Dev Cell 14*, 365-376.

4. Nazarko, T. Y., Farre, J. C., and Subramani, S. (2009) Peroxisome size provides insights into the function of autophagy-related proteins, *Mol Biol Cell 20*, 3828-3839.

Chapter IV: Rppa09976 mutants

Material and Methods

Strains

Pichia pastoris strains used in this study are described in Table 2-1.

Fluorescence Microscopy

Cells were grown in two pre-cultures of YPD, washed twice with YNB and transferred to peroxisome-induction medium with a starting OD_{600} of 0.3 for 15 h. To monitor localization of proteins by fluorescence microscopy, 100 ul of methanol-induced cells were collected and kept on ice before observation. Optimal exposition time for both the GFP and BFP fluorophores were used for each picture. Images were captured using a motorized fluorescence microscope (Axioskop 2 MOT; Carl Zeiss MicroImaging, Jena, Germany), coupled to a monochrome digital camera (AxioCam MRm; Carl Zeiss MiroImaging) and processed using the AxioVision 4.5 (Carl Zeiss MicroImaging) and Adobe Photoshop 7.0 software (Adobe Systems, Mountain View, CA).

Macropexophagy Assay

Cells were pre-grown in two pre-cultures of YPD. Cells were washed once with YNB solution and transferred to 25 ml of peroxisome-induction medium with a starting 0.3 OD_{600} for 15 h. Then, cells were washed twice with YNB solution and transferred to 25 ml of macropexophagy medium (1.7 g/l YNB without amino acids, 0.5% vol/vol ethanol) with a starting OD_{600} 2.0 for 0, 6, 9 and 12 h. Cells from 1 ml of culture were

collected and pelleted for each strain at each time point. Crude extracts were prepared in the presence of TCA and SDS-PAGE was performed as described previously.

mCherry-Atg8 Immunoprecipitation

25 OD of cells induced in micropexophagy conditions were pelleted and resuspended in 250 ul of IP buffer containing 0.5% vol/vol NP40, 50 mM HEPES-KOH pH 7.4, 50 mM NaCl, 1 mM EDTA, 10% vol/vol glycerol, 10 mM NaF and protease inhibitors (1 mM PMSF, 1 mM protease inhibitor cocktail, 1 mM leupeptin, and 1 mM aprotinin). Cell debris was removed by centrifugation at 21000 g for 10 min. The cell lysate was incubated 1 h at 4°C with 50 ul of washed GammaBind G Sepharose, to pre-clear the lysate of proteins that bind Sepharose nonspecifically. 10 ul of pre-cleared lysate was taken as input and diluted 20 times, and mixed with 200 ul of 2X SDS loading buffer and boiled for 5 min. The remaining 240 ul of pre-cleared lysate was incubated overnight at 4°C with 10 ul of DsRed polyclonal antibody (Living Colors). In order to pull-down mCherry-Atg8 bound to antibody, 50 ul of washed GammaBind G Sepharose was added to the lysate and incubated 1 h at 4°C. GammaBind G Sepharose was washed three times with IP buffer. Bound mCherry-Atg8 was eluted with 50 ul of 2X SDS loading buffer and boiled for 5 min prior to SDS-PAGE and western blotting (1). Each lane was loaded with 20 ul sample, as follows: Input 0.05 OD equivalent and IP mCherry-Atg8 9.6 OD equivalent.

Results

A. Construction of mutated versions of Rppa09976

Rppa09976 contains three putative Atg8 binding sites or **LC3** Interacting Regions (LIR motifs), a conserved acyl-CoA binding site and two transmembrane domains (Figure 2-1). It has been shown that point mutation of putative bulky residues of the LIR motifs to alanine leads to loss of Atg8 binding of selective autophagy receptors (2). Using site-directed mutagenesis we mutated all three LIR motifs, which hereafter we refer to 1st LIR (Y25A, L28A), 2nd LIR (W119A, I122A) and 3rd LIR (Y198A, L201A). We also made double mutants of the 2nd and 1st LIRs, as well as the 2nd and 3rd LIRs combined. Using site-directed mutagenesis we also mutated the conserved acyl-CoA binding site (Y40F and K44A) and two transmembrane domains (TMD). The acyl-CoA binding site which is composed of phenolyic hydroxyl group and tyrosine has been shown to be essential for acyl-CoA binding (3).

B. Mutant Rppa09976-GFP with either a mutated 2nd LIR or acyl-CoA binding site localizes to peroxisomes whereas Rppa09976-GFP lacking transmembrane domains is cytosolic

As described previously, Rppa09976 interacts with Pex3 and localizes to peroxisomes after one hour of methanol adaptation. Prior to checking effects of mutations on pexophagy and binding of Atg8, we checked the localization of these mutants using fluorescence microscopy. Colocalization of Rppa09976-GFP with BFP-SKL (peroxisomal marker) indicates correct peroxisomal localization of the mutated Rppa09976-GFP. Rppa09976-GFP mutated in either the 2nd LIR or acyl-CoA binding site localized to peroxisomes, whereas ΔTMD Rppa09976-GFP was cytosolic (Figure 4-1).

This showed that the point mutations do not affect localization of Rppa09976 hence can be used to study pexophagy and binding.

C. Rppa09976-GFP mutants are defective in pexophagy

We followed the levels of AOX (peroxisomal matrix protein) in a 12 hour time course as a readout of macropexophagy. We have previously shown that deletion of Rppa09976 leads to a block in pexophagy as AOX levels do not decrease over time, as they do in WT cells. Point mutations of the 2nd LIR and acyl-CoA binding sites, as well as deletion of transmembrane domains, led to block in macropexophagy (Figure 4-2).

D. Rppa09976-HA mutated at the 2nd LIR still interacts with mCherry-Atg8

We tested whether the 2nd LIR mutation blocked pexophagy due to the loss of Atg8 interaction. We immunoprecipitated mCherry-Atg8 under micropexophagy conditions and looked for co-immunoprecipitated Rppa09976-HA. This showed interaction of Atg8 and Rppa09976-HA (Figure 4-3, A) in both mutated and WT strains. Rppa09976-HA with its 2nd LIR mutated showed higher stability and ran at a higher molecular weight compared to WT Rppa09976-HA. Point mutation of two amino acids (W119A, I122A) could not account for such a large shift in molecular weight. This shift also led to an overlap in the migration of the mutant Rppa09976-HA with the heavy chain of antibody (mCherry) detected in the western blot of co-immunoprecipitates (Figure 4-3, A). We hypothesized that the shift might be due to hyperphosphorylation of the mutant Rppa09976-HA. However, the mutated Rppa09976-HA had higher molecular weight,

compared to WT Rppa09976-HA, even after 1 h induction in methanol medium, when the Rppa09976 protein is expected to be unmodified. Moreover, it accumulated modifications analogous to the modified forms of the non-mutated form of Rppa09976-HA at subsequent time-points (Figure 4-3, B).

E. The 1st and 2nd LIRs of Rppa09976 are redundant for binding to Atg8

Since mutation of the 2nd LIR did not abolish Atg8 binding, we checked the 1st and 3rd LIR mutants. We also checked the combination of 1st and 3rd mutants with the 2nd LIR mutant because the Rppa09976-HA fusion mutated in the 2nd LIR is more stable and easier to detect upon co-immunoprecipitation. The 1st and 3rd LIR mutations did not abolish Atg8 binding as shown by co-immunoprecipitation of Rppa09976-HA with mCherry-Atg8 (Figure 4-4, A). The 1st and 2nd LIR double mutant showed significantly lower co-immunoprecipitation of Rppa09976-HA compared to the 2nd LIR mutant alone or the double mutant with the 3rd and 2nd LIRs mutated (Figure 4-4, B), suggesting the requirement of both 1st and 2nd LIRs in binding of Rppa09976-HA to Atg8. Since the 1st LIR seemed important in Atg8 binding, the pexophagy assay was done. This mutant was defective in degradation of AOX, like the Δ*rppa09976* mutant, which indicated defective pexophagy (Figure 4-5).

Discussion

As predicted, Rppa09976 is a peroxisome membrane-bound protein which might provide acyl-CoA for growing isolation membranes that sequester peroxisomes. Recently, it has been shown that overexpression of cytosolic acyl-CoA protein leads to

faster formation of autophagosomes (4). In *P. pastoris*, Rppa09976 might have been evolved to provide acyl-CoA for large peroxisomes which are induced under methanol adaptation and might require significant amount of acyl-CoA for formation of isolation membrane. Recently, our lab also found that the double knockout of a cytosolic acyl-CoA binding protein and Rppa09976 show a stronger block in pexophagy than either of single knockout. It is of particular interest to know if this double knockout is also blocked in non-selective autophagy.

Based on co-immunoprecipitation of Rppa09976-HA with mCherry-Atg8, we cannot draw a firm conclusion on the requirement of LIR motifs of Rppa09976 for binding Atg8; however, the 1st and 2nd LIR seem to be important for binding to Atg8 as the double mutant has significantly lower affinity for Atg8. Additionally, single mutants of either the 1st and 2nd LIR are blocked in pexophagy. Perhaps, mutation of two residues is not sufficient for complete loss of interaction. Moreover, the 3rd LIR might also interact with Atg8 in which the first two LIRs are mutated. Resolution of this question will requires construction of a triple mutant lacking all three LIRs.

Chapter 4 is currently being prepared to submit for publication of the material. Lotfi, Pouya; Ozeki, Katharine; Nazarko, Taras Y; and Subramani, Suresh. The thesis author and Ozeki, Kahtherine contributed equally to this paper.

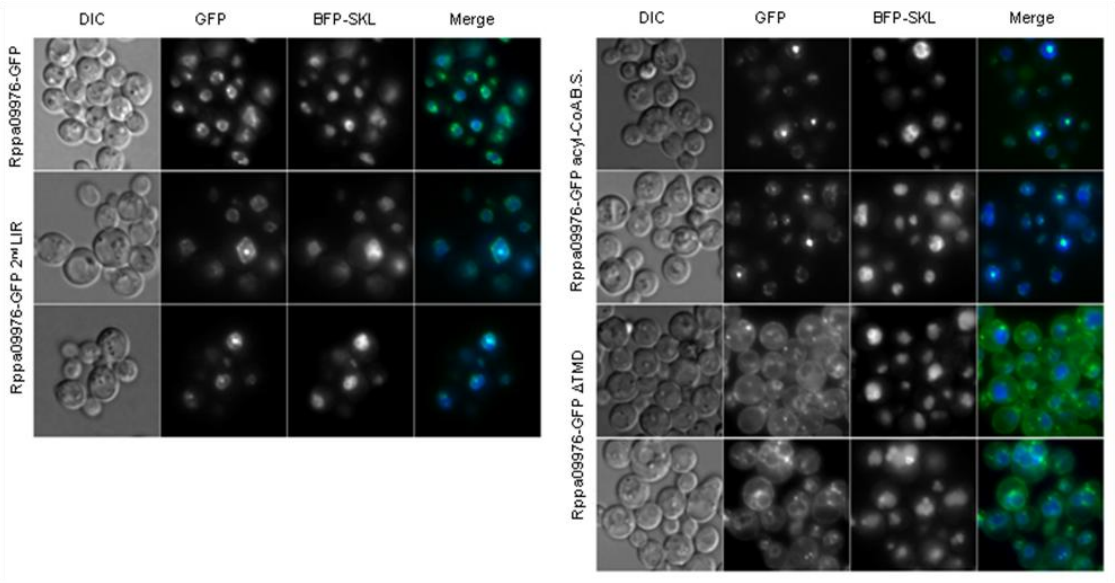

Figure 4-1: Localization of mutated versions of Rppa09976 in peroxisome-biogenesis conditions. Δ*rppa09976* Cells expressing either Rppa09976-GFP (STN151), Rppa09976-GFP with its 2nd LIR mutated (STN298, STN299), Rppa09976-GFP acyl-CoA binding site (B.S.) mutated (STN300, STN301), or Rppa09976-GFP ΔTMD (STN294, STN295). All strains expressed BFP-SKL (peroxisomal marker) and were grown in methanol medium for 15 h.

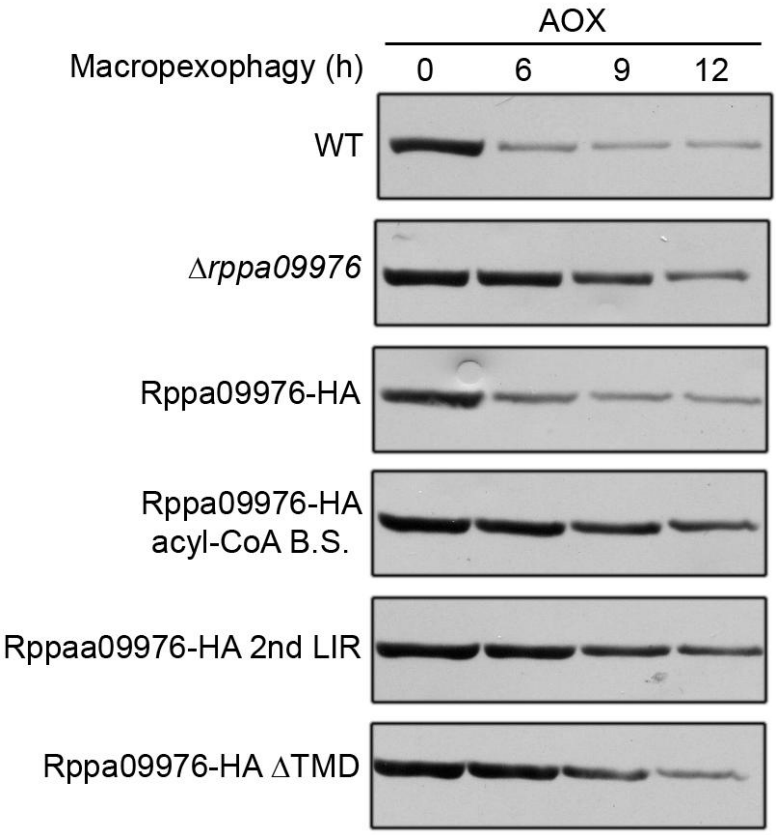

Figure 4-2: Pexophagy assay of mutated versions of Rppa09976. WT cells (PPY12h), Δ*rppa09976* (STN96), Δ*rppa09976* cells expressing Rppa09976-HA (STN215), Δ*rppa09976* cells expressing Rppa09976-HA acyl-CoA binding site (B.S.) mutated (STN292), Δ*rppa09976* cells expressing Rppa09976-HA 2nd LIR mutated (STN365), and Δ*rppa09976* cells expressing Rppa09976-HA ΔTMD (STN296). All strains were grown for 16 h in methanol medium and transferred to ethanol medium for 12 h.

A

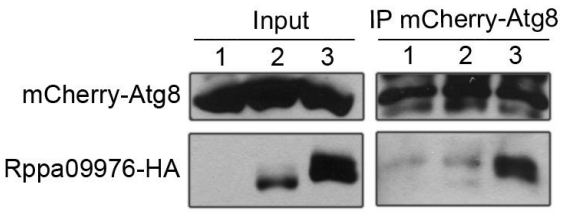

B

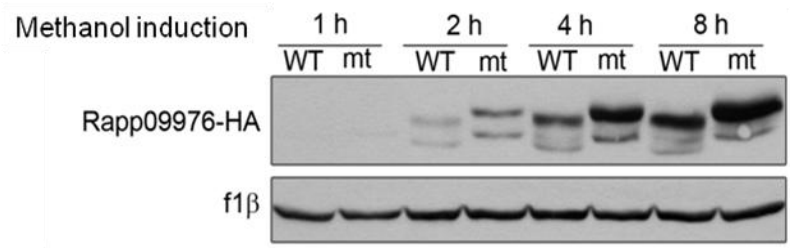

Figure 4-3: Co-immunoprecipition of Rppa09976-HA with mCherry-Atg8 under micropexophagy conditions. (A) Δ*rppa09976* cells (lane 1, STN362), Δ*rppa09976* cells expressing Rppa09976-HA (lane 2, STN363), Δ*rppa09976* cells expressing Rppa09976-HA 2nd LIR mutated (lane 3, STN365). All strains were induced for 16 h in methanol medium and transferred for 0.5 h to glucose medium. All strains expressed mCherry-Atg8. Immunoprecipitation was performed as described in Materials and Methods. (B) Δ*rppa09976* cells expressing Rppa09976-HA (WT, STN363) and Δ*rppa09976* cells expressing Rppa09976-HA 2nd LIR mutated (mt, STN365) were induced in methanol medium. The F1β subunit of mitochondrial ATPase was used as a protein loading control.

A

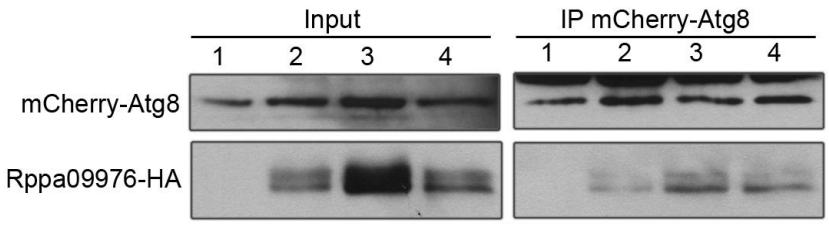

B

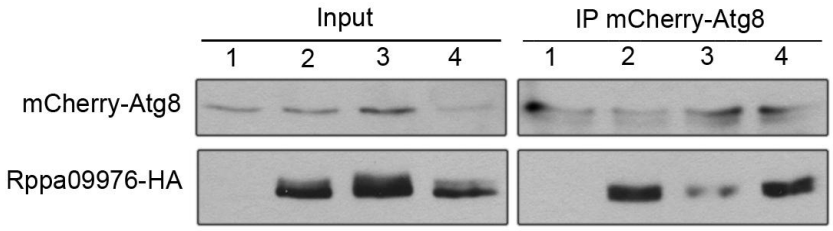

Figure 4-4: Co-immunoprecipition of single and double mutated LIR Rppa09976-HA with mCherry-Atg8 under micropexophagy conditions. (A) Δ*rppa09976* cells (lane 1, STN362), Δ*rppa09976* cells expressing Rppa09976-HA (lane 2, STN363), Δ*rppa09976* cells expressing Rppa09976-HA 1st LIR mutated (lane 3, STN462) and Δ*rppa09976* cells expressing Rppa09976-HA 3rd LIR mutated (lane 4, STN422). (B) Δ*rppa09976* cells (lane 1, STN362), Δ*rppa09976* cells expressing Rppa09976-HA 2nd LIR mutated (lane 2, STN365), Δ*rppa09976* cells expressing Rppa09976-HA 2nd and 1st LIR mutated (lane 3, STN420) and Δ*rppa09976* cells expressing Rppa09976-HA 2nd and 3rd LIR mutated (lane 4, STN424). All strains were induced for 16 h in methanol medium and transferred for 0.5 h to glucose medium. All strains expressed mCherry-Atg8. Immunoprecipitation was performed as described in Materials and Methods.

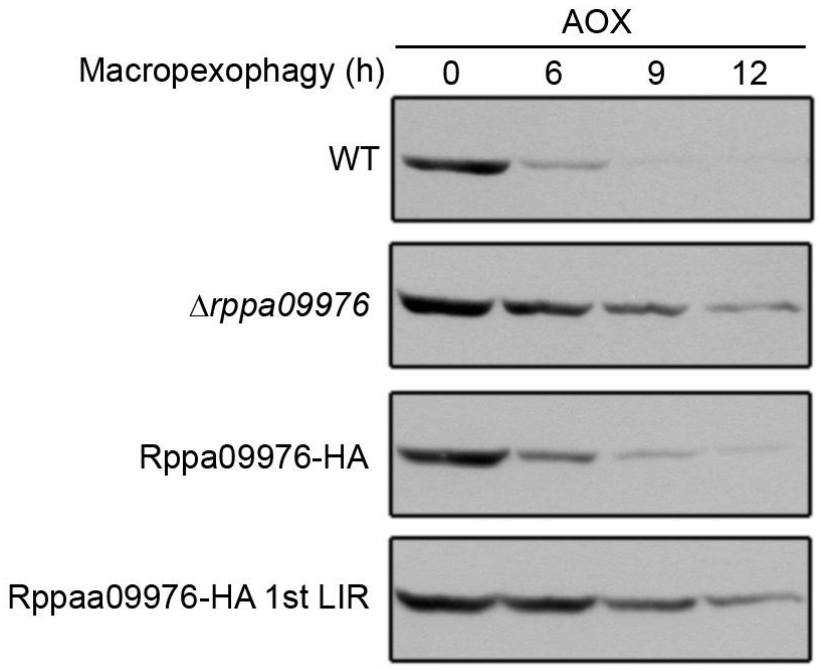

Figure 4-5: Pexophagy assay of 1st LIR mutated Rppa09976-HA. WT cells (PPY12h), Δ*rppa09976* (STN96), Δ*rppa09976* cells expressing Rppa09976-HA (STN215) and Δ*rppa09976* cells expressing Rppa09976-HA 1st LIR mutated (STN420). All strains were grown for 16 h in methanol medium and transferred to ethanol medium for 12 h.

References

1. Laemmli, U. K. (1970) Cleavage of structural proteins during the assembly of the head of bacteriophage T4, *Nature 227*, 680-685.

2. Noda, N. N., Kumeta, H., Nakatogawa, H., Satoo, K., Adachi, W., Ishii, J., Fujioka, Y., Ohsumi, Y., and Inagaki, F. (2008) Structural basis of target recognition by Atg8/LC3 during selective autophagy, *Genes Cells 13*, 1211-1218.

3. Kragelund, B. B., Knudsen, J., and Poulsen, F. M. (1999) Acyl-coenzyme A binding protein (ACBP), *Biochim Biophys Acta 1441*, 150-161.

4. Xiao, S., Gao, W., Chen, Q. F., Chan, S. W., Zheng, S. X., Ma, J., Wang, M., Welti, R., and Chye, M. L. (2010) Overexpression of Arabidopsis Acyl-CoA Binding Protein ACBP3 Promotes Starvation-Induced and Age-Dependent Leaf Senescence, *Plant Cell*.

Chapter V: Conclusion

Previous studies indicated Atg30 is the receptor for pexophagy, which interacts with the autophagic machinery as well as peroxisomal membrane. However, unlike other selective autophagy receptors, Atg30 does not interact with Atg8, the major component of the isolation membranes that sequester peroxisomes during pexophagy. Here, we found the missing link, a novel peroxisomal membrane protein Rppa09976, which acts as the co-receptor for pexophagy and bridges peroxisomes and Atg30 to the growing isolation membrane.

Rppa09976 encodes a 44 kDa protein containing an N-terminal acyl-CoA binding domain including a conserved acyl-CoA binding site, two transmembrane domains and three potential Atg8 binding motifs (LIR). Rppa09976 is induced upon methanol adaptation, and initially localizes at the endoplasmic reticulum (ER), then is delivered to peroxisomes, where it accumulates multiple phosphorylations. Mass spectrometry analysis of Rppa09976 revealed 21 phosphorylated residues. Rppa09976 is phosphorylated under peroxisome-biogenesis conditions even though it functions under pexophagy condition. Therefore, the role of phosphorylation remains unclear.

Mutational analysis of Rppa09976 revealed that defect in pexophagy is observed upon point mutation of the acyl-CoA binding site, the 1st and 2nd LIRs of Rppa09976 and deletion of transmembrane domains. The defect in pexophagy of the transmembrane domain mutant is due to mislocalization of Rppa09976, whereas defect in pexophagy of acyl-CoA binding site mutant might be due to the loss of binding to acyl-CoA, since it normally localizes to peroxisomes. The Rppa09976 with mutation of the 2nd LIR is

puzzling because even though it interacts with Atg8 and localizes to peroxisomes, it is still defective in pexophagy. Mutation of the 1st LIR has the same effect as mutation of the 2nd LIR, however combination of these mutations leads to significant loss of Atg8 interaction. A triple mutant might be required for complete loss of Atg8 interaction.

Using co-immunoprecipitation we also found Rppa09976 interacts with Pex3 and Atg30 under micropexophagy conditions. Fluorescence microscopy results of peroxisomal localization of these proteins illustrate that Rppa09976 localization depends on Atg30, and localization of Pex3 and Atg8 depends on Rppa09976 and Atg30. Microscopy results are in agreement with biochemical data that Rppa09976 is downstream of Atg30 linking peroxisomal membrane to isolation membrane for the following reasons: 1) Rppa09976 localization is dependent on Atg30, and not vice versa; 2) Rppa09976 interacts with Atg8, but Atg30 does not.

Colocalization studies of Rppa09976 and Atg8 show that Rppa09976 is concentrated at the regions of peroxisomes where MIPA tips are growing whereas Atg8 is seen throughout MIPA. Hence, Rppa09976 might act in a zippering mechanism where it would donate acyl-CoA necessary for elongation of isolation membrane that sequesters peroxisomes.

Chapter 5 is currently being prepared to submit for publication of the material. Lotfi, Pouya; Ozeki, Katharine; Nazarko, Taras Y; and Subramani, Suresh. The thesis author and Ozeki, Kahtherine contributed equally to this paper.